Design, Synthesis, and Evaluation of An Anti-trypanosomal [1,2,4]Triazolo[1,5-*a*]pyrimidine Probe for Photoaffinity Labeling Studies

Bobby Lucero,[a] Karol R. Francisco,[a, b] Carmine Varricchio,[c] Lawrence J. Liu,[a, b] Yuemang Yao,[e] Andrea Brancale,[d] Kurt R. Brunden,[e] Conor R. Caffrey,*[b] and Carlo Ballatore*[b]

Studies have shown that depending on the substitution pattern, microtubule (MT)-targeting 1,2,4-triazolo[1,5-*a*]pyrimidines (TPDs) can produce different cellular responses in mammalian cells that may be due to these compounds interacting with distinct binding sites within the MT structure. Selected TPDs are also potently bioactive against the causative agent of human African trypanosomiasis, *Trypanosoma brucei*, both *in vitro* and *in vivo*. So far, however, there has been no direct evidence of tubulin engagement by these TPDs in *T. brucei*. Therefore, to enable further investigation of anti-trypanosomal TPDs, a TPD derivative amenable to photoaffinity labeling (PAL) was designed, synthesized, and evaluated in PAL experiments using HEK293 cells and *T. brucei*. The data arising confirmed specific labeling of *T. brucei* tubulin. In addition, proteomic data revealed differences in the labeling profiles of tubulin between HEK293 and *T. brucei*, suggesting structural differences between the TPD binding site(s) in mammalian and trypanosomal tubulin.

Introduction

The microtubule (MT)-targeting [1,2,4]triazolo[1,5-*a*]pyrimidines (TPDs) are a class of synthetic compounds that elicit one of three different responses in mammalian cells (HEK293).[1–3] For "Class I" TPDs, changes in the substituents linked at the C6 and/or C7 position of the TPD core result in compounds that stabilize MTs without altering total tubulin levels (*e.g.*, **1**, Figure 1A).[1,3] By contrast, "Class II" TPDs generate a bell-shaped concentration effect regarding MT-stabilization, and trigger proteasome-dependent degradation of tubulin (*e.g.*, **2** in Figure 1A).[1,3] The third group, called "hybrid" TPDs (*e.g.*, **3**, Figure 1A), are similar to Class II compounds in producing a bell-shaped concentration response in cellular assays of MT-stabilization, but like Class I TPDs do not cause changes in total tubulin levels.[2]

Co-crystal structure studies[4,5] conducted with mammalian tubulin preparations and representative examples of Class I (**1**) and II (**2**) TPDs revealed that the different effects of these compounds on MTs may stem from the fact that these TPDs interact with MTs at either one or two structurally related interfacial binding sites; specifically, the seventh site[5] (or gatorbulin site[6]), which is present within individual α,β-tubulin heterodimers, and/or the vinca site, which is between two longitudinally associated heterodimers. Whereas modeling suggests that the Class I TPDs interact predominantly within the vinca binding site, resulting in stabilization of MTs, the Class II TPDs appear to interact with similar affinity with both the vinca and the seventh sites.[2] Moreover, X-ray data suggests that the interaction of Class II TPDs within the seventh site results in the displacement of the non-exchangeable GTP nucleotide that results in misfolding and degradation of tubulin.[5] No co-crystal structures involving hybrid TPDs have been solved to date. However, computational studies suggest that these compounds, like the Class II TPDs, interact with both the vinca and the seventh sites with similar affinity.[2]

A recent study of a broad set of TPD derivatives from all three classes against *Trypanosoma brucei in vitro* indicated that

[a] *B. Lucero, K. R. Francisco, L. J. Liu*
Department of Chemistry and Biochemistry
University of California, San Diego
9500 Gilman Drive, La Jolla, CA 92093, USA

[b] *K. R. Francisco, L. J. Liu, Prof. C. R. Caffrey, Prof. C. Ballatore*
Center for Discovery and Innovation in Parasitic Diseases
Skaggs School of Pharmacy and Pharmaceutical Sciences
University of California, San Diego
9500 Gilman Drive, La Jolla, CA 92093, USA
E-mail: cballatore@health.ucsd.edu
ccaffrey@health.ucsd.edu

[c] *C. Varricchio*
School of Pharmacy and Pharmaceutical Sciences
Cardiff University
Cardiff CF103NB, U.K.

[d] *A. Brancale*
Vysoká Škola Chemicko-Technologická v Praze
Department of Organic Chemistry
Technická 5, Prague 16628, Czech Republic

[e] *Y. Yao, K. R. Brunden*
Center for Neurodegenerative Disease Research
Perelman School of Medicine
University of Pennsylvania
3600 Spruce Street, Philadelphia, Pennsylvania 19104, USA

Supporting information for this article is available on the WWW under https://doi.org/10.1002/cmdc.202300656

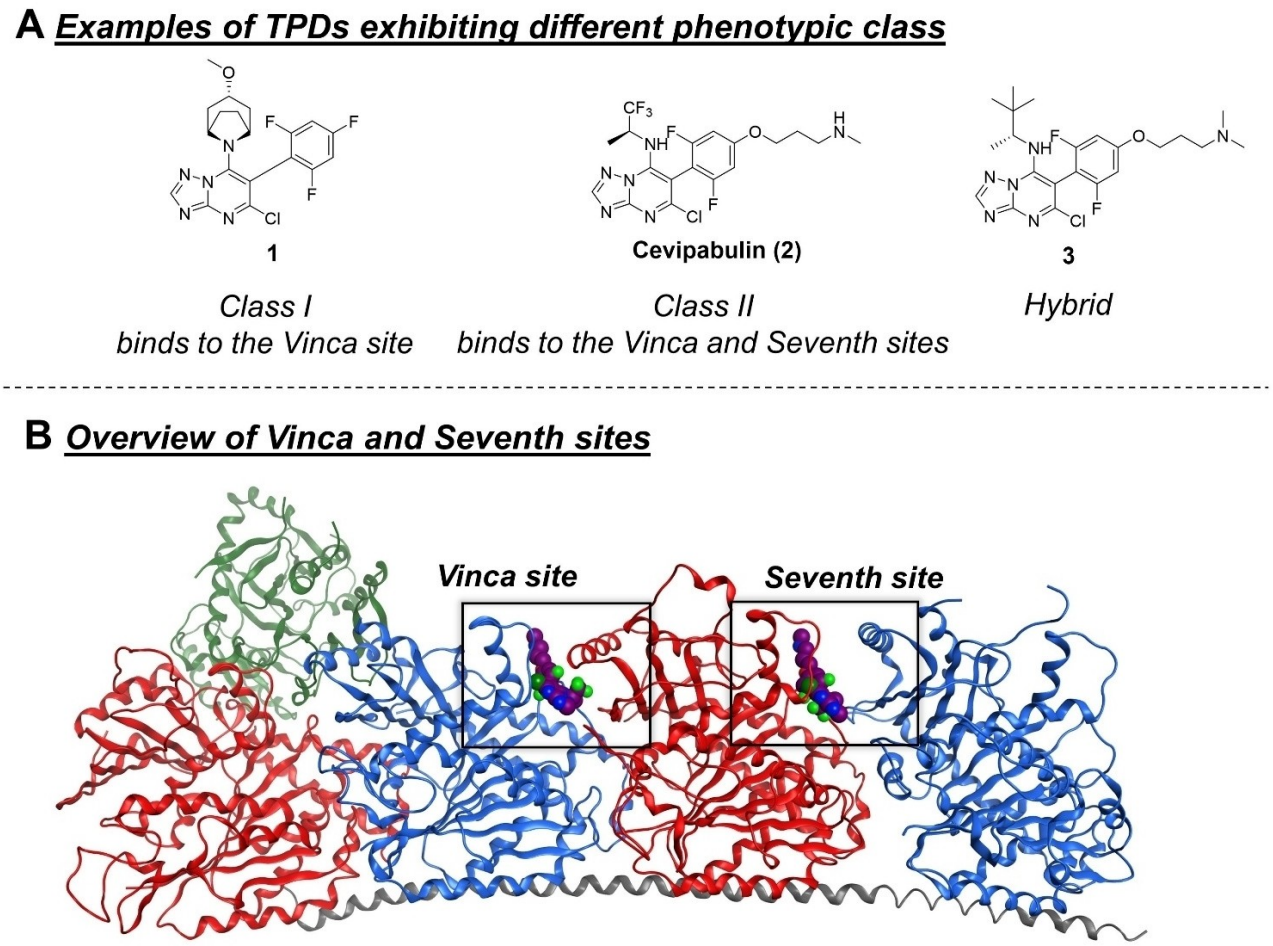

Figure 1. (A) Chemical structures of representative Class I (**1**), Class II (**2**) and hybrid (**3**) TPDs. (B) Co-crystal structure of TPD **2** (purple) bound to two binding sites, the vinca and the seventh site. α-tubulin (red), β-tubulin (blue), tubulin tyrosine ligase (green), stathmin-like protein RB3 (grey). PDB: 7CLD.[5]

hybrid and Class II TPDs are potent nanomolar anti-trypanosomal compounds.[7] In addition, although these compounds did not show cell selectivity *in vitro*, short-term treatments (*i.e.*, single- or two-dose treatments) of *T. brucei*-infected mice with selected hybrid or Class II TPDs at or below the maximum tolerated dose decreased parasitemia to below detectable levels which translated into a significant extension of mouse survival.[7] Furthermore, a comparison of a matched molecular pair of representative compounds from the hybrid and Class II TPDs indicated that hybrid TPDs may provide a more promising combination of efficacy and tolerability *in vivo*.[7] Although these results indicate that hybrid TPDs might be potential candidates to treat African trypanosomiasis, thus far, there has been no direct evidence of *T. brucei* tubulin engagement by TPDs. Towards this end, and to allow for future investigations into possible differences between the structures of vinca and seventh sites in mammalian and *T. brucei* that could be exploited to design compounds with selectivity to trypanosomal tubulin, we developed a photoactivatable probe derived from the hybrid TPD, **3**, and used this compound in photoaffinity labeling (PAL) experiments with HEK293 cells and *T. brucei*. The results indicate that the hybrid TPD probe labels both α- and β-tubulin in *T. brucei*, whereas in HEK293 cells, labeling involves almost exclusively β-tubulin. These results provide direct evidence of tubulin engagement by TPDs in *T. brucei*. Moreover, the different labeling profiles in *T. brucei* and HEK293 cells suggest that structural differences exist between the TPD binding site(s) of trypanosomal and mammalian tubulin/MTs. These findings provide impetus for future studies that will explore whether structural differences within mammalian and trypanosomal tubulin/MTs might be exploited to design more potent and/or selective anti-trypanosomal TPDs.

Results and Discussion

The design of the hybrid TPD PAL probe (Figure 2A) took advantage of our previous findings that photoreactive alkyl diazirines may be tolerated as replacements of the small alkyl group of the amine fragment at C7, resulting in TPD derivatives that retain comparable activity as the parent compounds in the cell-based assay.[8] Based on these prior results, we expected that the *t*-butyl group of **3** could be substituted with a diazirine ring resulting in a photoreactive derivative with activities comparable to the parent compound.

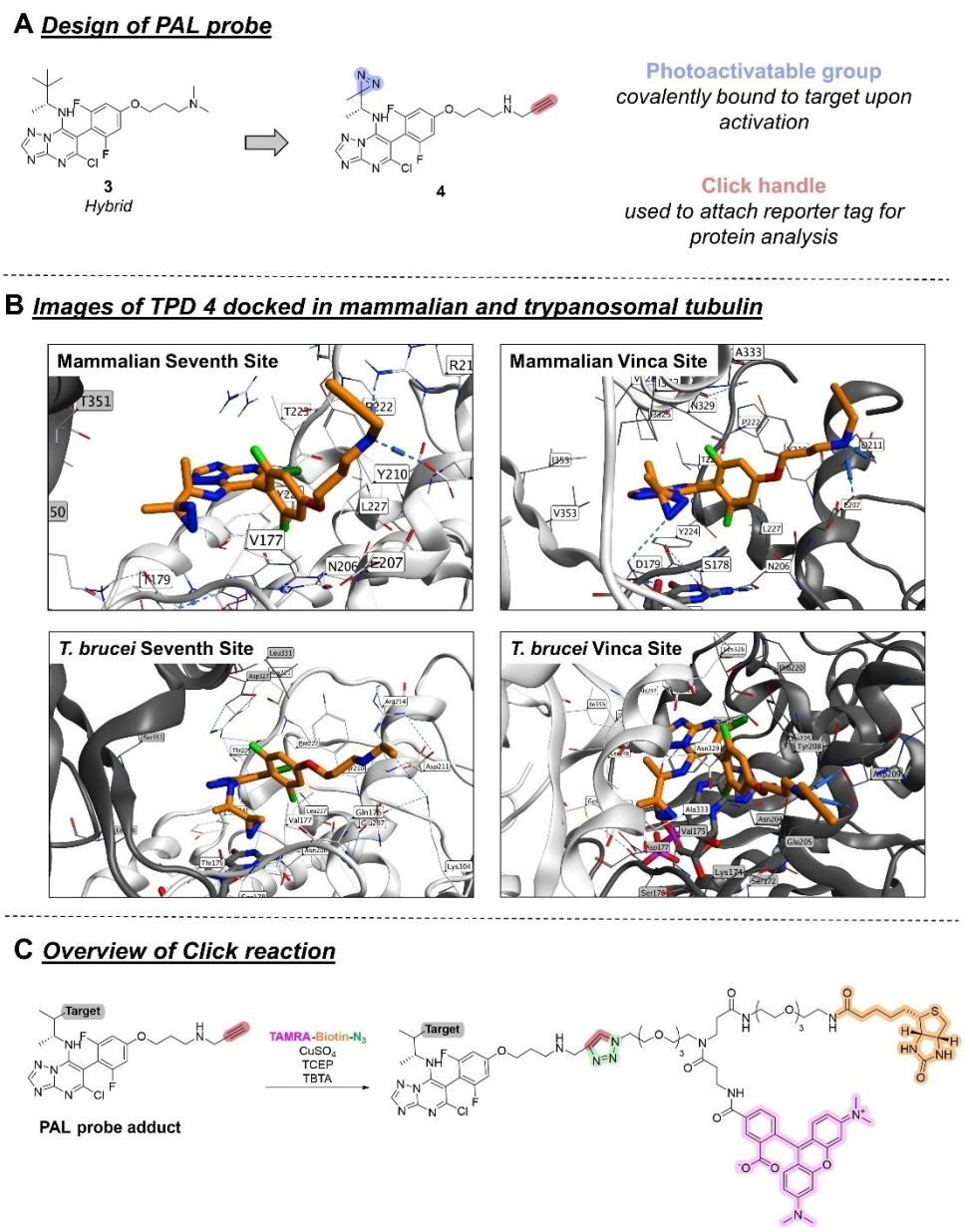

Figure 2. (A) The chemical structure of TPD PAL probe, **4**, which was derived from the hybrid TPD, **3**. (B) Docking of **4** to the seventh and vinca sites of mammalian tubulin (vinca site, from PDB: 5NJH;[4] seventh site, from PDB: 7CLD)[5] and to *T. brucei* tubulin (homology model); α-tubulin is shown in light-gray and β-tubulin in dark-gray. (C) Overview of the click reaction used after photolabeling of protein(s) to install the fluorescence (TAMRA) and affinity (biotin) tags.

Further, to enable a PAL workflow that would be based upon the one described by Taunton and co-workers[9] which involves post-photolabeling click reactions with a conjugate bearing both a biotin and a fluorescent reporter, the candidate TPD probe was equipped with a terminal alkyne handle (Figure 2A & C). Docking studies with the candidate TPD probe (Figure 2B and Table 1) indicated that the presence of the diazirine ring at C7 and the alkyne handle at the end of the alkoxy side-chain would result in a TPD probe which, like **3**, would exhibit similar affinities for the vinca and seventh sites in both mammalian and *T. brucei* MTs.

The synthesis of the PAL probe **4** (Scheme 1) was conducted by adopting established strategies for the synthesis of TPDs[2,3] and their diazirine-containing derivatives.[8] Thus, starting from the TPD di-chloride **5**,[2] chemoselective displacement of the chloride at C7 by the diazirine-containing amine fragment (**6**) led to intermediate **7**. Next, incorporation of the alkoxide side-chain via nucleophilic substitution provided TPD **8**, which, after reaction with TMS-propargyl aldehyde under reductive amination conditions (**9**) and subsequent desilylation, furnished the desired compound **4**.

After synthesis, the TPD derivative was incubated at 1 or 10 μM in a 4 h cell-based MT assay,[1] after which acetylated α-

Table 1. MT-Stabilizing Activity, HEK293 Cytotoxicity, and Anti-Trypanosomal Activity of Test Compounds.

Cpd	Structure	MT-stabilization assay[b] (HEK293 cells)				HEK293 CC_{50} (nM)[c]	*T. brucei* EC_{50} (nM)[d]	Calc. Binding Energy[e] ΔG (kcal/mol)	
		AcTub		α-Tub					
		1 μM	10 μM	1 μM	10 μM			Vinca site mammalian (*T. brucei*)	Seventh site mammalian (*T. brucei*)
3[a]	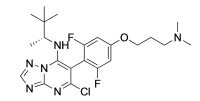	6.75 ± 0.32**	2.99 ± 0.02**	0.97 ± 0.06	0.97 ± 0.03	10.8 ± 1.5	38.9 ± 5.3	−60.11 (−62.84)	−62.13 (−54.40)
4	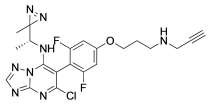	10.3 ± 0.1**	2.69 ± 0.20**	0.97 ± 0.04	1.08 ± 0.06	64.6 ± 9.4	265.3 ± 44.8	−62.79 (−55.46)	−60.64 (−57.85)

[a] Data previously published.[2,7] [b] Fold-changes in acetylated α-tubulin (AcTub) and total α-tubulin (α-Tub) protein levels in HEK293 cells, relative to vehicle (DMSO)-treated cells, were determined after a 4 h incubation with compound at either 1 or 10 μM (*$p < 0.05$ and **$p < 0.01$ by one-way ANOVA). [c] Cytotoxicity was measured using HEK293 cells and a resazurin cell viability assay.[10] Cells were incubated for 48 h with compound and the CC_{50} values calculated using GraphPad Prism (sigmoidal 4PL). Assays were performed as three experimental replicates, each as a singleton, and the means ± SD values are shown. [d] Antitrypanosomal activity was measured using a resazurin cell viability assay.[10,11] *T. brucei brucei* Lister 427 parasites were incubated for 72 h in the presence of compound and EC_{50} values calculated using GraphPad Prism (sigmoidal 4PL). Assays were performed as three biological replicates in duplicate, and the means ± SD values are shown. [e] Calculated binding energy from docking studies at the seventh and vinca sites of mammalian tubulin and *T. brucei* tubulin (values in brackets). The mammalian vinca and seventh sites are from PDB: 5NJH[4] and PDB: 7CLD[5], respectively, whereas the corresponding sites in *T. brucei* tubulin are based on homology modeling.

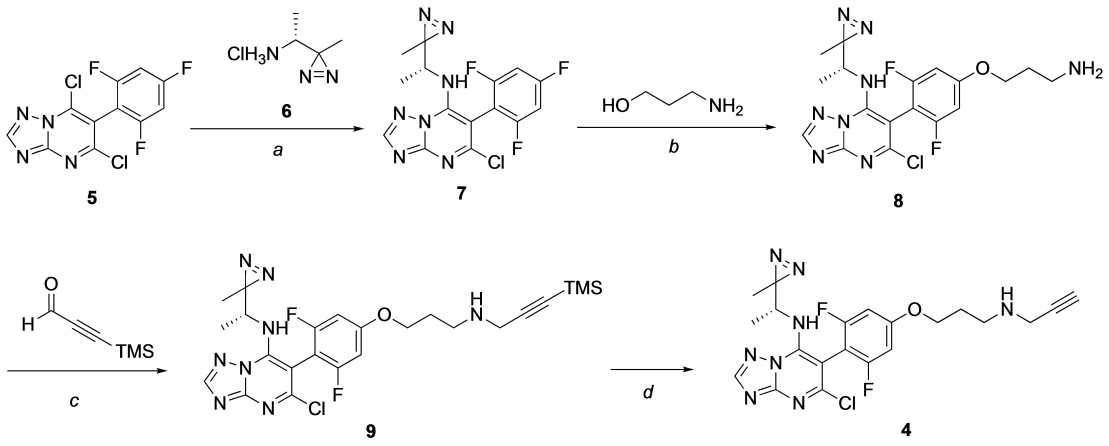

Scheme 1. Synthesis of PAL probe **4**. *Reagents and conditions*: (a) (*R*)-1-(3-methyl-3H-diazirin-3-yl)ethan-1-amine hydrochloride,[5] Et_3N, DMF, 1 h, rt, 78%; (b) 3-aminopropan-1-ol, NaH, DMSO, 60 °C, 6 h, 87%; (c) 3-(trimethylsilyl)propiolaldehyde, MeOH, 0 °C 3 h, followed by $NaBH_4$, 25% ; (d) K_2CO_3, MeOH, 2 h, rt, 84%.

tubulin (AcTub), a known cellular marker for stable MTs, and total α-tubulin levels were determined by ELISA in cell lysates.[1] The candidate probe was also tested *in vitro* for cytotoxicity against HEK293 cells and activity against *T. brucei brucei* Lister 427 (Table 1). As summarized in Table 1, the activity of the probe in the cell-based assays appeared to be similar to that of the parent TPD. In the HEK293 MT-stabilization assay, TPD probe **4** elicited similar effects on tubulin as measured for the hybrid TPD **3**, with increases in the acetylation of α-tubulin that were comparatively lower after compound incubation at 10 μM than at 1 μM (~2.7× *vs.* 10.3× respectively), but without causing meaningful changes in total tubulin levels. Furthermore, although the activity of the probe in both the HEK293 and *T. brucei* assays was ~six-fold lower than the parent TPD, the CC_{50} and EC_{50} values of **4** remained in the sub-μM range. Thus, the overall activity of the probe appeared to be qualitatively and quantitatively appropriate for PAL studies.

To define the optimal conditions for the PAL experiments, *i.e.*, the time required for photoactivation and the click reaction, and the click reaction temperature, a series of preliminary experiments (Figure 3A) was conducted using purified porcine brain tubulin (Cytoskeleton, cat. T240). From these studies, a PAL workflow was established (Figure 3A). Tubulin was first incubated with the probe for 30 min, followed by photoactivation at 365 nm (for 30 min) using a hand-held UV-lamp that was kept at approximately 3–10 mm from the mixture. After photoactivation, the mixture was subjected to the click reaction for 30 min at 37 °C (Supporting Information) to attach a conjugate containing both a fluorescence reporter and an affinity tag (TAMRA-Biotin-N_3, Figure 2B). Finally, the protein

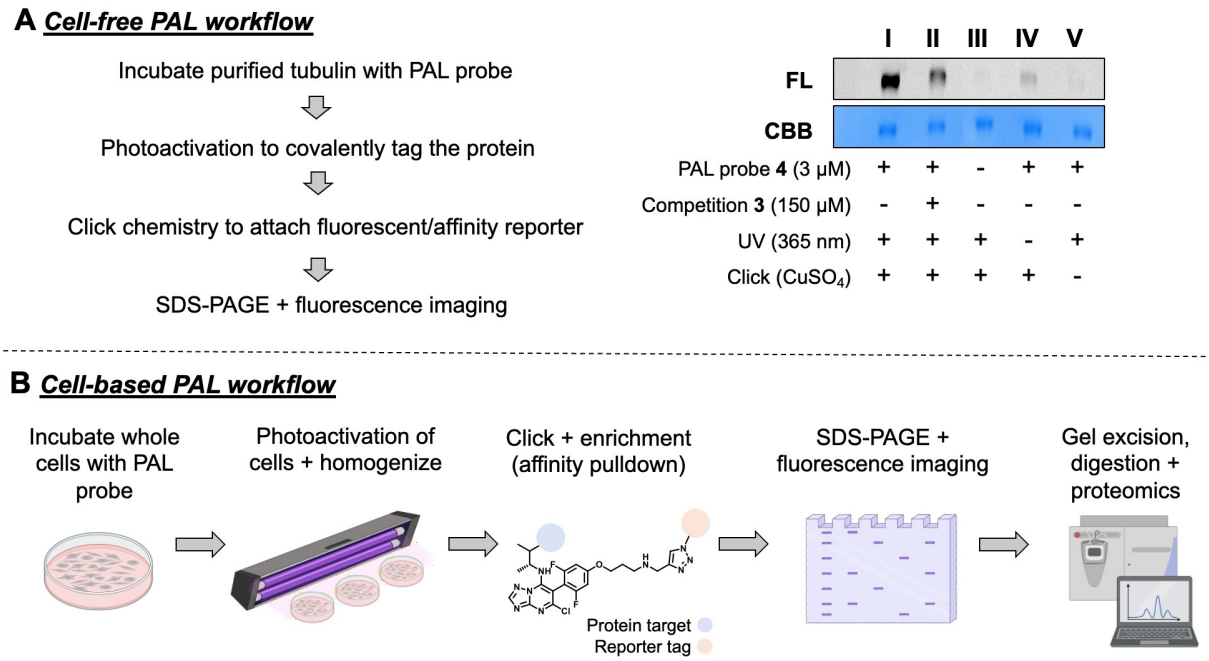

Figure 3. A) Cell-free PAL workflow involves 1) incubation of purified tubulin (3 μM) with the PAL probe (3 μM) for 30 min at 37 °C; 2) photoactivation (30 min) of the protein-probe mixture to covalently bind the PAL probe to the protein; 3) click chemistry (30 min at 37 °C) to attach the combined fluorescence and affinity tag to the PAL probe-protein adduct; and 4) SDS-PAGE to separate excess reagents from the protein and visualization of the tagging via fluorescence imaging. In addition to the standard PAL conditions as described (I), competition experiments including 50-fold excess photostable Hybrid TPD **3** (II) were conducted revealing a reduction of ~64% of fluorescence signal as determined by densitometry. Control experiments including: no PAL probe (III); no photoactivation (IV) and no click catalyst (V) were also carried out. Staining of SDS-PAGE gel by Coomassie Brilliant Blue indicated approximately equal protein loading. (B) Overview of cell-based PAL workflow. Whole cells were incubated with the PAL probe followed by photoactivation. The cells were then collected, washed and homogenized, and the resulting lysates were reacted *in situ* via a click reaction with TAMRA-Biotin-N_3, followed by biotin affinity purification, SDS-PAGE and fluorescence imaging. Finally, the fluorescent SDS-PAGE bands were excised, digested, and subjected to proteomics analysis. PAL = photoaffinity labeling; FL = fluorescence; CBB=Coomassie brilliant blue.

was separated from the click reagents via SDS-PAGE, and protein labeling by the probe was analyzed via fluorescence imaging. Competition studies with the photostable TPD **3**, and the implementation of various control experiments (Figure 3A), confirmed the specific interaction of the PAL probe with tubulin. Accordingly, these experimental conditions were applied to PAL studies involving HEK293 cells and *T. brucei*.

Experiments with HEK293 cells (Figure 3B) involved an initial incubation with 3 μM of the PAL probe for 4 h (*i.e.*, the same incubation time as the MT-stabilizing assay),[1] followed by UV irradiation of cells for 30 min. Cells were then collected, washed with PBS and sonicated. The protein content of the cell lysates was quantified using a BCA assay (protein concentration of 0.2–0.8 mg/mL). The lysates were subjected to the click reaction with TAMRA-Biotin-N_3 followed by SDS-PAGE, and the gel analyzed via fluorescence. A prominent fluorescent band at ~50 kDa, which corresponds to the MW of tubulin, as well as bands of lower fluorescent intensity were resolved (Figure 4A).

Due to their faster growth rate compared to HEK293 cells doubling time of (6–8 *vs.* 24 h), a lower PAL probe concentration of 0.3 μM and a shorter incubation time of 2 h were used for the PAL experiments with *T. brucei* to ensure that the PAL experiments were conducted under conditions that would not cause death of the parasites. Otherwise, the protocol was the same as described for the HEK293 cells. Again, a prominent fluorescent band at ~50 kDa was observed, as was a second band at ~40 kDa (Figure 4B). As shown in Figure 4A, B and the Supporting Information, a 20× excess of **3** relative to the PAL probe decreased the fluorescence of the ~50 kDa band in both HEK293 cells and *T. brucei* by approximately 95% and 46% respectively, indicating specific labeling events. For the HEK293 cells, the competition with **3** also produced a partial but significant reduction of the fluorescent intensity of the bands at ~30 and ~70 kDa (Figure 4A). In contrast, for *T. brucei*, the fluorescence intensity of the ~40 kDa band was not reduced by an excess of **3**, suggesting the possibility of non-specific labeling (Figure 4B).

Finally, to enable proteomic analysis of the proteins labeled, lysates were subjected to biotin-affinity purification prior to SDS-PAGE, and different bands of interest (highlighted with red brackets in Figure 4A and B) were then excised and analyzed by proteomics (LC–MS/MS). These studies confirmed that the bands at ~50 kDa are highly abundant in tubulin. However, whereas ~99% of all the tubulin labeled in HEK293 cells consisted of different isoforms of β-tubulin (Figure 5A), the photolabeling resulted in nearly equal tagging of α- and β-tubulin in *T. brucei*, (Figure 5B). Taken together, these results demonstrate that the hybrid TPD, **4**, interacts specifically with trypanosomal tubulin. Further, although mammalian and *T. brucei* tubulin share >80% amino acid sequence identity, the different labeling ratios of α- and β-tubulin observed between

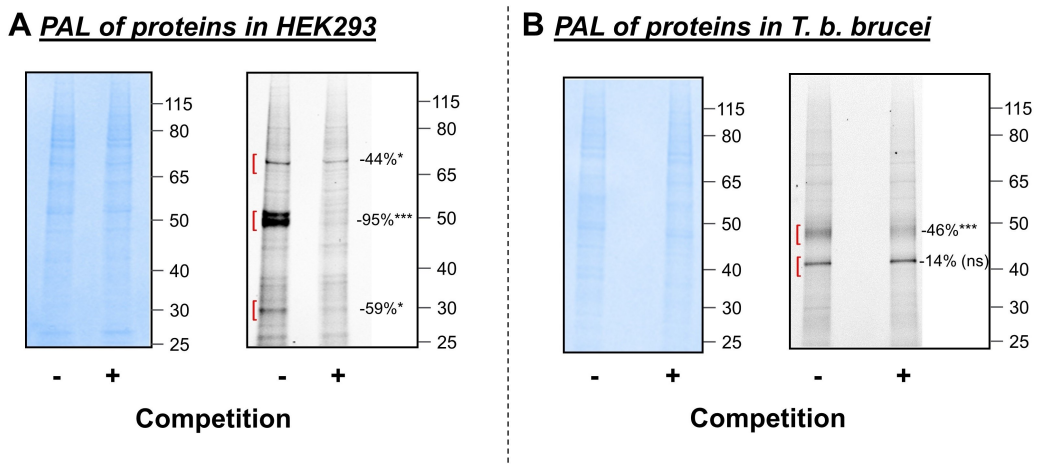

Figure 4. TAMRA-based fluorescence of proteins bound by PAL probe **4** in extracts of HEK293 cells and *T. b. brucei* Lister 427. (A) For HEK293 cells, binding by **4** the 50 kDa band (−) was decreased by 95%*** by prior incubation with 20x excess of the photostable TPD, **3** (+): the fluorescence of two additional bands at 70 and 30 kDa was also significantly decreased by 44%* and 59%*, respectively. (B) For *T. brucei*, the fluorescent band at 50 kDa (−) was significantly decreased by 46%*** in the presence of **3**, whereas the intensity of a second band at 40 kDa was not altered by competition (14%, ns). Percent competition was calculated using densitometry analysis (*$p < 0.05$; ***$p < 0.001$ using the unpaired *t*-test).

the parasite and mammalian tubulin suggest structural differences in the TPD binding sites.

Apart from tubulin being identified as a specific binder, the PAL experiments in HEK293 cells also indicated labeling events of other proteins at approximately ~70 kDa and ~30 kDa that could be competed for with **3**. Proteomic analysis of the excised bands determined that the band at ~70 kDa comprises members of the 70 kDa heat shock protein (HSP70) family of molecular chaperones, namely the 71 kDa heat shock cognate, and the 70 kDa heat shock proteins, as well as the RNA-binding protein, nucleolin. The labeled ~30 kDa band in HEK293 cells contained 40S and 60S ribosomal proteins, as well as the high mobility group protein B1. For *T. brucei*, the 40 kDa band comprised peptides identifying glyceraldehyde 3-phosphate dehydrogenase, arginine kinase, 60S ribosomal protein and asparagine synthethase a. Although these proteins have been reported as potential targets for drug development,[12] the significance of these data in the context of TPDs is unclear as the lack of competition with an excess of TPD **3** suggests that the labeling of these proteins may have resulted from non-specific binding by the probe TPD.

Conclusions

Based on the design and implementation of PAL protocols described herein, we provide direct evidence that hybrid TPDs engage tubulin in both a representative mammalian cell line, HEK293, and in *T. brucei*. Also, comparison of the PAL data arising from the HEK293 cells and *T. brucei* suggest possible structural differences between the TPD binding site(s) in trypanosomal and mammalian tubulin/MTs. Further studies will determine whether these differences can be targeted to design TPD derivatives with improved selectivity to *T. brucei*.

Experimental Section

Chemistry

Materials and Methods: All solvents and reagents were reagent grade and used as received. Thin layer chromatography (TLC) was performed using 200 μM MilliporeSigma precoated silica gel aluminum sheets. Flash chromatography was performed with SiliaFlash P60 (particle size 40–63 μM) supplied by Silicycle. ^{1}H and ^{13}C NMR spectra were recorded on a 600 MHz NMR spectrometer. Chemical shifts were reported relative to residual solvent's peak. HPLC purifications were performed using a SunFire preparative C18 OBD column (5 μm 19×50 mm) on a Gilson instrument. Samples were analyzed with analytical HPLC and employed 10% to 90% of CH_3CN in H_2O over 6–12 min and flow rate of 2 mL/min. Samples purified by preparative HPLC employed 10% to 90% of CH_3CN in H_2O over 6–20 min and flow rate of 20 mL/min. All final compounds were found to be > 95% pure by LC/MS.

(*R*)-5-Chloro-*N*-(1-(3-methyl-3H-diazirin-3-yl)ethyl)-6-(2,4,6-trifluorophenyl)-[1,2,4]triazolo[1,5-*a*]pyrimidin-7-amine (**7**). Intermediate **7** was synthesized according to published procedure[5] with spectra matching literature.

(*R*)-6-(4-(3-Aminopropoxy)-2,6-difluorophenyl)-5-chloro-*N*-(1-(3-methyl-3H-diazirin-3-yl)ethyl)-[1,2,4]triazolo[1,5-*a*]pyrimidin-7-amine (**8**). To a suspension of NaH (60 wt% in mineral oil) (0.051 g, 0.68 mmol, 4.00 eq) in anhydrous DMSO (2.00 mL, 0.35 M) was added 3-aminopropan-1-ol (0.027 g, 0.68 mmol, 4.00 eq). The reaction was stirred at 60 °C for 30 min. Then, a solution of **7** in anhydrous DMSO (0.52 M) was added at 60 °C and stirred for 6 h in the dark. The reaction was quenched at rt with satd. sodium bicarbonate and extracted (3X) with EtOAc. The combined organic layers were washed with satd. aq. NaCl, dried over $MgSO_4$, filtered and concentrated. Purification via silica gel chromatography (20–80% EtOAc/Hexanes) furnished the desired compound **8** (0.065 g, 0.15 mmol, 87%). ^{1}H NMR (600 MHz, MeOD) δ 8.44 (s, 1H), 6.83 (dd, $J = 14.8$, 10.6 Hz, 2H), 4.19 (t, $J = 6.1$ Hz, 2H), 3.35 (s, 1H), 2.97 (t, $J = 7.1$ Hz, 2H), 2.07 (m, 2H), 1.00 (d, $J = 6.8$ Hz, 3H), 0.90 (s, 3H) ppm.

(*R*)-5-Chloro-6-(2,6-difluoro-4-(3-((3-(trimethylsilyl)prop-2-yn-1-yl)amino)propoxy)phenyl)-*N*-(1-(3-methyl-3H-diazirin-3-yl)ethyl)-[1,2,4]triazolo[1,5-*a*]pyrimidin-7-amine (**9**). To a solution of amine **8**

A ***Proteomic analysis of bands excised from SDS-PAGE gel (HEK293)***

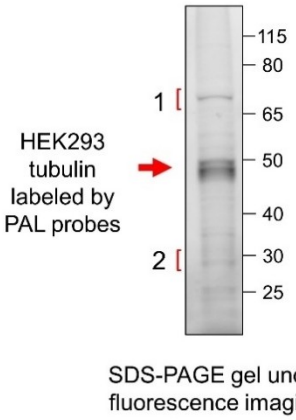

Protein	-10LogP[a]	% of Total Tubulin[b]
Tubulin β-5 chain	358.74	83.93
Tubulin β-4B chain	353.43	10.87
Tubulin β-2B chain	346.89	0.90
Tubulin β-2A chain	345.48	0.67
Tubulin β-4A chain	344.09	0.28
Tubulin β-3 chain	328.38	0.51
Tubulin β-6 chain	309.38	1.55
Tubulin α-1C chain	290.23	0.72
Tubulin α-4A chain	278.76	0.04
Tubulin β-8 chain	265.46	0.51
Tubulin β-8B chain	256.46	0.01

B ***Proteomic analysis of bands excised from SDS-PAGE gel (T. brucei)***

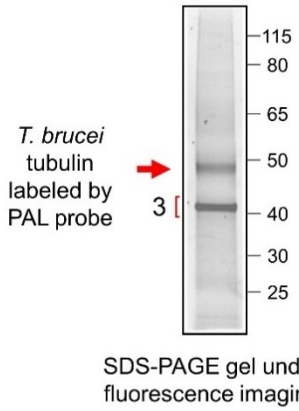

Protein	-10LogP[a]	% of Total Tubulin[b]
β Tubulin	697.78	43.55
α Tubulin	657.06	56.45

C ***Proteomic analysis of bands 1 & 2 (HEK293), and 3 (T. brucei)***

Cell Line	Band	% Competition[c]	Protein	Protein Mass (Da)	-10LogP[a]
HEK293	1	-44%	Heat shock cognate 71 kDa	70898	236.32
			Heat shock 70 kDa	70109	216.19
			Nucleolin	76615	194.17
HEK293	2	-59%	High mobility group protein B1	24894	233.13
			60S ribosomal protein	29226	209.58
			40S ribosomal protein	29598	195.31
T. brucei	3	-14%	glyceraldehyde 3-phosphate dehydrogenase glycosomal	43869	501.22
			arginine kinase	40197	392.42
			60S ribosomal protein	41856	368.86
			asparagine synthetase a	39597	349.81

Figure 5. Proteomic analysis of proteins enriched for by the biotin-functionality of PAL probe **4** in extracts of HEK293 cells and *T. b. brucei* Lister 427. Labeling of tubulin by **4** was confirmed for HEK293 cells (A) and the parasite (B). (C) Proteomic analysis of non-tubulin bands that were labeled by **4** in HEK293 cells and in *T. brucei*. [a]PEAKS peptide scores (−10logP) indicate high confidence in the identity of proteins present. [b]Percent peak area of each tubulin isoform relative to all tubulin isoforms present in the sample. [c]Percent competition, as determined in the experiment shown in Figure 4, represents the % reduction in TAMRA-based fluorescence of proteins caused by photostable TPD **3**.

(0.065 g, 0.15 mmol, 1.00 eq) in MeOH (0.20 mL, 0.80 M) cooled to 0 °C was added 3-(trimethylsilyl)propiolaldehyde (0.019 mg, 0.15 mmol, 1.00 eq) and the resulting mixture was stirred for 3 h. while maintaining 0 °C. Sodium borohydride (0.011 g, 0.30 mmol, 2.00 eq) was added portionwise over 30 min and then the mixture was stirred for 1 h allowing the temperature to raise to rt. The reaction was then quenched with 5% sodium bicarbonate and the resulting mixture was extracted (3X) with EtOAc. The combined organic extracts were washed with water, satd. aq. NaCl, dried with $MgSO_4$, filtered and concentrated. Purification via silica gel chromatography (20–80% EtOAc/Hexanes) furnished the desired compound **9** (0.020 g, 0.037 mmol, 25%). ^{1}H NMR (600 MHz, $CDCl_3$)

δ 8.35 (s, 1H), 6.65 (m, 2H), 4.14 (t, J = 6.1 Hz, 2H), 2.94 (t, J = 6.7 Hz, 2H), 2.06 (m, 2H), 1.24 (s, 2H), 0.90 (s, 3H), 0.86 (d, J = 6.9 Hz, 3H), 0.16 (d, J = 2.5 Hz, 8H) ppm.

(*R*)-5-Chloro-6-(2,6-difluoro-4-(3-(prop-2-yn-1-ylamino)propoxy)phenyl)-*N*-(1-(3-methyl-3H-diazirin-3-yl)ethyl)-[1,2,4]triazolo[1,5-a]pyrimidin-7-amine (**4**). To a solution of **9** (0.020 g, 0.037 mmol, 1.00 eq) in MeOH (0.25 mL, 0.1 M) was added Na_2CO_3 (0.015 g, 0.15 mmol, 4.00 eq) and the resulting mixture was stirred for 1 h. The reaction was then filtered and purified by reverse-phase HPLC (10 to 90% ACN in H_2O, 0.1% formic acid) obtaining the desired compound **4** (0.016 g, 0.031 mmol, 84%). ^{1}H NMR (600 MHz, $CDCl_3$) δ 8.37 (s, 1H), 8.23 (s, 1H), 6.70 – 6.61 (m, 2H), 5.93 (d, J = 9.8 Hz, 1H), 4.17 (t, J = 5.8 Hz, 2H), 3.73 (d, J = 2.5 Hz, 2H), 3.22 (t, J = 7.0 Hz, 2H), 2.45 (d, J = 2.5 Hz, 1H), 2.25 (p, J = 6.6 Hz, 2H), 0.92 (s, 2H), 0.89 (d, J = 6.8 Hz, 3H) ppm. HRMS (ES^+): calcd for $C_{21}H_{22}ClF_2N_8O$ $[M+H]^+$, 461.1411; found, 461.1412.

In silico studies

Computational studies were conducted using MAESTRO (Schrödinger)[13] and the Molecular Operating Environment (MOE).[14] The αβ-tubulin complex with cevipabulin was obtained from the Protein Data Bank (PDB ID: 7CLD), while the homology model for *T. brucei* tubulin was constructed as described in our recent study[7]. Briefly, the FASTA sequences for α- (P04106) and β- (P04107) tubulin from the UniProt database were used to model the proteins based on the mammalian tubulin structure (PDB: 7CLD[5]) and refined with the AMBER10: EHT force field using MOE 2022.02. Preparation of both proteins was conducted using the Protein Preparation Wizard in MAESTRO. All co-crystallized molecules except for the ligand and GDP were removed, and the protonation states of protein residues were assessed at 300 K and pH 7. A 15 Å docking grid (inner box, 10 Å; outer box, 20 Å) was prepared using as centroid the co-crystallized ligands. TPD compounds were prepared considering ionization states at pH 7 ± 2. The docking studies were performed using with Glide SP precision, keeping default parameters. The docking results were further refined using the Prime module's MMGBSA approach in Maestro. Finally, protein-ligand interaction analyses and visual inspections were performed using MOE 2022.2.

Cell Culture and in vitro Assays

Cell Culture. HEK293 cells were cultured in DMEM supplemented with 10% heat-inactivated FBS and 1% penicillin-streptomycin. Cells were grown in T75 cell culture flasks maintained at 37 °C in 5% CO_2 and sub-cultured when at 60–80% cell confluence. Bloodstream forms of *T. b. brucei* Lister 427 were grown in HMI-9 medium[15] in T25 suspension cell culture flasks at 37 °C in 5% CO_2, as described.[10,11] Trypanosomes were maintained in exponential growth phase and passaged every 48–72 h.

HEK293 MT-stabilization and Cytotoxicity Assays. The assessment of the stable MT marker, AcTub, in compound-treated HEK293 cells was as previously described.[1–3] Cytotoxicity in HEK293 cells was measured using a resazurin cell viability assay.[16] Test compounds were serially diluted in DMSO and added to 96-well polystyrene assay plates to give final assay concentrations ranging from 20 μM to 0.87 nM (1 μL; 1% total DMSO). Fresh medium was added to the assay plate (49 μL/well). HEK293 cells were suspended to 4×10^5 cells/mL in DMEM and added to each well (50 μL) for a total density of 2×10^4 cells/well. Assay plates were incubated at 37 °C and 5% CO_2 for 48 h, followed by addition of 20 μL 0.5 mM resazurin (Alfa Aesar, Cat. B21187) in PBS to each well. Assay plates were incubated in the dark for 2 h at 37 °C. Fluorescence was measured at 531 nm and 595 nm excitation and emission wavelengths, respectively, using a 2104 EnVision® multilabel plate reader. The viability of each well was normalized to positive and negative controls in each assay plate. Dose-response curves were generated and EC_{50} values calculated with GraphPad Prism, version 9.3 (San Diego, CA) using a sigmoidal four parameter logistic curve.

T. brucei Cell Viability Assay. Growth inhibition of *T. b. brucei* Lister 427 was determined using a resazurin cell viability assay.[10] Test compounds were serially diluted in DMSO and added to 96-well polystyrene assay plates to give final assay concentrations ranging from 20 μM to 0.87 nM (1 μL; 0.5% total DMSO). Fresh HMI-9 medium (99 μL/well) was added to the assay plate. Parasites in exponential phase were suspended at 2×10^5 parasites/mL in HMI-9 medium and added to each well (100 μL) to a total density of 2×10^4 trypanosomes/well. Assay plates were incubated at 37 °C and 5% CO_2 for 72 h, followed by addition of 20 μL 0.5 mM resazurin (Alfa Aesar, Cat. B21187) in PBS to each well. Assay plates were incubated in the dark for 2 h at 37 °C. Fluorescence was measured at 531 nm and 595 nm excitation and emission wavelengths, respectively, using a 2104 EnVision® multilabel plate reader. The viability of each well was normalized to positive and negative controls in each assay plate. Dose-response curves were generated as described for HEK293.

Photoaffinity Labeling

HEK293 Incubation with PAL Probe. HEK293 cells ($1–5\times10^5$ cells) were seeded on 60×15 mm plates and used when cells were 70–90% confluent. The medium was removed and replaced with 5 mL medium containing the PAL probe/TPD competitor (less than 0.5% DMSO). The cells in plates (no lids) were exposed for 30 min to a 365 nm light source positioned at a distance of 1–2 cm. After photoactivation, the medium was removed, and the cells were washed once with PBS. Cells were detached from the plates using 0.05% Trypsin-EDTA and then diluted with medium. The cells were centrifuged, washed 3x with PBS and frozen at −80 °C.

T. brucei Incubation with the PAL Probe. A 12.5 mL suspension of *T. b. brucei* Lister 427 in log-phase growth ($2–4\times10^6$ parasites/mL) was mixed with an equal volume of medium containing the desired PAL probe/TPD competitor (less than 0.5% DMSO). The parasites were incubated at 37 °C and 5% CO_2 for 2 h. The parasite suspension was transferred to 60×15 mm plates (no lids), and then exposed for 30 min to a 365 nm light source positioned at a distance of 1–2 cm. The cells were then centrifuged, washed 3x with PBS, and frozen at −80 °C.

Homogenization, Protein Quantification, Click Chemistry. Cells were collected and lysed in PBS (200 μL) in the presence of 1× protease inhibitor cocktail without EDTA (Fisher Cat 78429), and the protein concentration was quantified by BCA assay using Pierce™ BCA Protein Assay Kit (ThermoFisher Cat# 23227) according to the manufacturer's instructions. The protein samples were diluted with PBS to ensure an equal protein concentration (approx. 0.2–0.8 mg/mL). To prepare for click chemistry,[17] 200 μL of the protein samples were reduced via addition of 25 μL 10% SDS solution (approximately 1% total SDS) followed by vortexing. Next, 5 μL of 5 mM solution of Biotin-TAMRA azide (Click Chemistry Tools Cat # 1048) in DMSO. The click catalyst mixture was freshly prepared containing 3 : 1 : 1 ratio of 1.7 mM Tris(benzyltriazolylmethyl)amine (TBTA)[18] (in 80% *t*-butanol and 20% DMSO), 50 mM $CuSO_4$ (in water), and 50 mM Tris (2-carboxyethyl) phosphine (TCEP) (in water), and then adjusted to pH 7 using 1 M NaOH. The click catalyst (25 μL) was added to the protein sample. The reaction mixtures were then incubated at 37 °C in an incubator for 30 mins.

SDS-PAGE and Fluorescence Imaging. SDS-PAGE analysis was performed to check for the efficiency of click labeling and analysis. Thirty μL of the resulting clicked protein samples were added to 10 μL 4X LDS sample loading buffer (Fisher Cat# NP0007) containing 10% 2-mercaptoethanol. The samples were denatured at 95 °C for 2 min and loaded on to a precast Bolt™ 1.00 mm, 4–12% Bis-Tris plus minigel. Electrophoresis employed a constant 120 V for 1.5 h. Gels were visualized by fluorescence imaging (excitation/emission: 546/578) using a Biorad ChemiDoc MP imaging system, and stained with Coomassie Brilliant Blue.

Affinity Purification. After the click reaction, the protein mixture was precipitated by the addition of three volumes of cold acetone and incubated in a −20 °C freezer for 30 min. The precipitated protein was centrifuged and the supernatant was aspirated. The pellet was washed with cold acetone, resuspended, and centrifuged twice more. After the final acetone wash, the resulting pellet was left to air dry and reconstituted in 1% SDS in PBS. Prewashed 50% Neutravidin agarose bead slurry (25 μL; Fisher Cat 29200) was added to each protein sample and incubated at room temperature for 2 h with constant end-over-end mixing. The mixture was then centrifuged and the supernatant discarded. The beads were washed with 0.1% tween in PBS (3×) and then with PBS (3×), discarding each supernatant after each wash. Affinity purified proteins bound to the beads were eluted by boiling in 1× LDS sample loading buffer for 5 min. The resulting mixture was separated via SDS-PAGE, visualized by fluorescence, and Coomassie-stained as described previously. The gel bands of interest were excised for proteomics analysis (LC–MS/MS).

In-Gel digest. The gel slices were cut into 1×1 mm cubes and destained three times by first washing with 100 μL of 100 mM ammonium bicarbonate for 15 min, followed by addition of the same volume of acetonitrile (ACN) for 15 min. The supernatant was removed and the samples dried in a speedvac. Samples were then reduced by mixing with 200 μL 100 mM ammonium bicarbonate containing 10 mM DTT and incubated at 56 °C for 30 min. The liquid was removed and 200 μL 100 mM ammonium bicarbonate containing 55 mM iodoacetamide was added to the gel pieces and incubated in the dark at room temperature for 20 min. After removal of the supernatant and one wash with 100 mM ammonium bicarbonate for 15 min, the same volume of ACN was added to dehydrate the gel pieces. The solution was then removed and the samples were dried in a speedvac. For digestion, enough solution of ice-cold trypsin (0.01 μg/μL) in 50 mM ammonium bicarbonate was added to cover the gel pieces and the reaction was left on ice for 30 min. After complete rehydration, the excess trypsin solution was removed, replaced with fresh 50 mM ammonium bicarbonate, and left overnight at 37 °C. The peptides were extracted twice by the addition of 50 μL 0.2% formic acid and 5% ACN, and vortexed at room temperature for 30 min. The supernatant was removed and saved. A total of 50 μL 50% ACN, 0.2% formic acid was added to the sample, which was vortexed again at room temperature for 30 min. The supernatant was removed and combined with the supernatant from the first extraction. The combined extractions were analyzed directly by liquid chromatography (LC) in combination with tandem mass spectroscopy (MS-MS) using electrospray ionization.

LC-MS-MS proteomics analysis. Trypsin-digested peptides were analyzed by ultra-high pressure liquid chromatography (UPLC) coupled with MS/MS using nano-spray ionization. The nanospray ionization experiments were performed using a Orbitrap fusion Lumos hybrid mass spectrometer (Thermo) interfaced with nano-scale reversed-phase UPLC (Thermo Dionex UltiMate™ 3000 RSLC nano System) using a 25 cm, 75-micron ID glass capillary packed with 1.7-μm C18 (130) BEHTM beads (Waters corporation). Peptides were eluted from the C18 column into the mass spectrometer using a linear gradient (5–80%) of ACN at a flow rate of 375 μL/min for 1 h. The buffers used to create the ACN gradient were: Buffer A (98% H2O, 2% ACN, 0.1% formic acid) and Buffer B (100% ACN, 0.1% formic acid). Data-dependent acquisition mode was used for the mass spectrometer and the mass spectrometer parameters were as follows; an MS1 survey scan using the orbitrap detector (mass range (m/z): 400–1500 (using quadrupole isolation), 60000 resolution setting, spray voltage of 2200 V, Ion transfer tube temperature of 275 °C, AGC target of 400000, and maximum injection time of 50 ms was followed by data-dependent scans (top speed for most intense ions), with the charge state set to only include +2–5 ions, and a 5 second exclusion time, while selecting ions with minimal intensities of 50000 at which the collision event was carried out in the high energy collision cell (HCD Collision Energy of 30%), and the fragment masses where analyzed in the ion trap mass analyzer (With ion trap scan rate of turbo, first mass m/z was 100, AGC Target 5000 and maximum injection time of 35 ms). Protein identification was carried out using Peaks Studio X (Bioinformatics solutions Inc.)

Acknowledgements

Financial support for this research was provided in part by the National Institute of Allergy and Infectious Diseases (NIAID) at the National Institutes of Health under award number R21AI141210. The content is solely the responsibility of the authors and does not necessarily represent the official views of the National Institutes of Health.

Conflict of Interests

The authors declare no conflict of interest.

Data Availability Statement

The data that support the findings of this study are available in the supplementary material of this article.

Keywords: African trypanosomiasis · triazolopyrimidines · photoaffinity labeling · *Trypanosoma brucei* · microtubules · vinca site · seventh site

[1] J. Kovalevich, A. S. Cornec, Y. Yao, M. James, A. Crowe, V. M. Lee, J. Q. Trojanowski, A. B. Smith, C. Ballatore, K. R. Brunden, *J. Pharmacol. Exp. Ther.* **2016**, *357*, 432–450.
[2] T. Alle, C. Varricchio, Y. Yao, B. Lucero, G. Nzou, S. Demuro, M. Muench, K. D. Vuong, K. Oukoloff, A. S. Cornec, K. R. Francisco, C. R. Caffrey, V. M. Lee, A. B. Smith, A. Brancale, K. R. Brunden, C. Ballatore, *J. Med. Chem.* **2023**, *66*, 435–459.
[3] K. Oukoloff, G. Nzou, C. Varricchio, B. Lucero, T. Alle, J. Kovalevich, L. Monti, A. Cornec, Y. Yao, M. James, J. Trojanowski, V. Lee, A. Smith, A. Brancale, K. Brunden, C. Ballatore, *J. Med. Chem.* **2021**, *64*, 1073–1102.
[4] G. Sáez-Calvo, A. Sharma, F. A. Balaguer, I. Barasoain, J. Rodríguez-Salarichs, N. Olieric, H. Muñoz-Hernández, M. Berbís, S. Wendeborn, M. A. Peñalva, R. Matesanz, Á. Canales, A. E. Prota, J. Jímenez-Barbero, J. M. Andreu, C. Lamberth, M. O. Steinmetz, J. F. Díaz, *Cell Chem. Biol.* **2017**, *24*, 737–750.e736.

[5] J. Yang, Y. Yu, Y. Li, W. Yan, H. Ye, L. Niu, M. Tang, Z. Wang, Z. Yang, H. Pei, H. Wei, M. Zhao, J. Wen, L. Yang, L. Ouyang, Y. Wei, Q. Chen, W. Li, L. Chen, *Sci. Adv*. **2021**, *7*.
[6] S. Matthew, Q. Y. Chen, R. Ratnayake, C. S. Fermaintt, D. Lucena-Agell, F. Bonato, A. E. Prota, S. T. Lim, X. Wang, J. F. Díaz, A. L. Risinger, V. J. Paul, M. Oliva, H. Luesch, *Proc. Natl. Acad. Sci. USA* **2021**, *118*, e2021847118.
[7] L. Monti, L. J. Liu, C. Varricchio, B. Lucero, T. Alle, W. Yang, I. Bem-Shalom, M. Gilson, K. R. Brunden, A. Brancale, C. R. Caffrey, C. Ballatore, *ChemMedChem* **2023**, *18*, e202300193.
[8] K. Oukoloff, J. Kovalevich, A. S. Cornec, Y. Yao, Z. A. Owyang, M. James, J. Q. Trojanowski, V. M. Lee, A. B. Smith, K. R. Brunden, C. Ballatore, *Bioorg. Med. Chem. Lett.* **2018**, *28*, 2180–2183.
[9] A. L. MacKinnon, J. Taunton, *Curr Protoc Chem Biol* **2009**, *1*, 55–73.
[10] K. R. Francisco, L. Monti, W. Yang, H. Park, L. J. Liu, K. Watkins, D. K. Amarasinghe, M. Nalli, C. Roberto Polaquini, L. O. Regasini, A. E. Miller Crotti, R. Silvestri, L. Guidi Magalhães, C. R. Caffrey, *Bioorg. Med. Chem. Lett.* **2023**, *81*, 129123.
[11] L. Monti, S. C. Wang, K. Oukoloff, A. B. Smith, K. R. Brunden, C. R. Caffrey, C. Ballatore, *ChemMedChem* **2018**, *13*, 1751–1754.
[12] a) A. J. Cáceres, P. A. Michels, V. Hannaert, *Mol. Biochem. Parasitol.* **2010**, *169*, 50–54; b) A. M. Aronov, S. Suresh, F. S. Buckner, W. C. Van Voorhis, C. L. Verlinde, F. R. Opperdoes, W. G. Hol, M. H. Gelb, *Proc. Natl. Acad. Sci. USA* **1999**, *96*, 4273–4278; c) M. Pandey, Y. Huang, T. K. Lim, Q. Lin, C. Y. He, *J. Biol. Chem.* **2020**, *295*, 11326–11336; d) C. P. Ooi, B. Rotureau, S. Gribaldo, C. Georgikou, D. Julkowska, T. Blisnick, S. Perrot, I. Subota, P. Bastin, *PLoS One* **2015**, *10*, e0133676; e) K. Prohaska, N. Williams, *Eukaryotic Cell* **2009**, *8*, 77–87; f) I. Loureiro, J. Faria, C. Clayton, S. M. Ribeiro, N. Roy, N. Santarém, J. Tavares, A. Cordeiro-da-Silva, *PLoS Neglected Trop. Dis.* **2013**, *7*, e2578.
[13] *Schrödinger Release 2022–3*: Glide, Schrödinger, LLC, New York, NY, **2021**.
[14] *Molecular Operating Environment (MOE)*, 2022.02 Chemical Computing Group ULC, Montreal, QC, Canada, H3 A 2R7, **2022**].
[15] H. Hirumi, K. Hirumi, *J. Parasitol.* **1989**, *75*, 985–989.
[16] J. O'Brien, I. Wilson, T. Orton, F. Pognan, *Eur. J. Biochem.* **2000**, *267*, 5421–5426.
[17] H. C. Kolb, K. B. Sharpless, *Drug Discovery Today* **2003**, *8*, 1128–1137.
[18] T. R. Chan, R. Hilgraf, K. B. Sharpless, V. V. Fokin, *Org. Lett.* **2004**, *6*, 2853–2855.

Manuscript received: November 22, 2023
Revised manuscript received: January 19, 2024
Accepted manuscript online: January 26, 2024
Version of record online: ■■, ■■

RESEARCH ARTICLE

We describe here the design, synthesis and evaluation of an anti-trypanosomal 1,2,4-triazolo[1,5-*a*]pyrimidine (TPD) probe which facilitated the design and execution of PAL experiments in whole HEK293 cells and *T. brucei* parasites. These experiments confirmed tubulin as a protein target in both HEK293 cells and *T. brucei.*

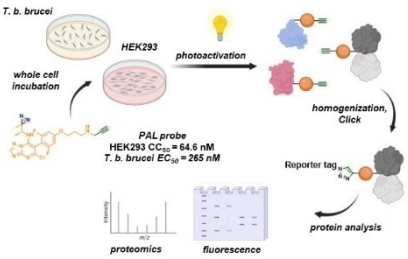

B. Lucero, K. R. Francisco, C. Varricchio, L. J. Liu, Y. Yao, A. Brancale, K. R. Brunden, Prof. C. R. Caffrey, Prof. C. Ballatore**

1 – 11

Design, Synthesis, and Evaluation of An Anti-trypanosomal [1,2,4]Triazolo[1,5-*a*]pyrimidine Probe for Photoaffinity Labeling Studies